Title: Seizure onset and offset pattern determine the entrainment of the cortex and substantia nigra in the nonhuman primate model of focal temporal lobe seizures

Running Title: Propagation of Temporal Lobe Seizure Patterns.

Authors: Mark J. Connolly[1,2], Sujin Jiang[3], Lim Samuel[3], Claire-Anne Gutekunst[4], Robert E. Gross[2,4,5], Annaelle Devergnas[†,1,5]

[1]Emory National Primate Research Center, Emory University, Atlanta, GA 30329, USA
[2]Wallace H. Coulter Department of Biomedical Engineering, Emory University and Georgia Institute of Technology, Atlanta, GA, 30332, USA
[3]Emory College of Arts & Sciences, Emory University, Atlanta, GA, 30322, USA
[4]Department of Neurosurgery, Emory University School of Medicine, Atlanta, GA, 30322, USA
[5]Department of Neurology, Emory University School of Medicine, Atlanta, GA, 30322, USA
[†]Corresponding

Corresponding author:
Annaelle Devergnas, PhD.
Emory National Primate Research Center
Emory University
954 Gatewood Road NE, Atlanta, GA 30329, USA.
Email: adeverg@emory.edu
Phone: 404-727-6305
Fax: 404-727-9294

Disclosures: Robert E. Gross serves as a consultant to Medtronic, which manufactures products related to the research described in this manuscript and receives compensation for these services. He also receives support for unrelated research. The terms of this arrangement have been reviewed and approved by Emory University in accordance with its conflict of interest policies.

Acknowledgements: This work was supported by The National Institutes of Health National Institute of Neurological Disorders and Stroke grant UG3-NS100559.

Abstract:

Temporal lobe (TL) epilepsy is the most common form of drug-resistant epilepsy. A major focus of human and animal studies on TLE network has been the limbic circuit and the structures composing the temporal lobe. However, there is also evidence suggesting an active role of the basal ganglia in the propagation and control of temporal lobe seizures. Evidence suggests that the network involved in temporal lobe seizure may depend on their onset and offset pattern but studies on the relationship between the patterns and extralimbic activity are limited. Here, we characterize the involvement of the substantia nigra (SN) and somatosensory cortex (SI) during temporal lobe seizures induced in two nonhuman primates (NHP). The seizure onset and offset patterns were manually classified and spectral power and coherence were calculated. We then analyzed the three first and last seconds of the seizure as well as 3-second segments of recorded in pre-ictal and post-ictal periods and compared the changes based on the seizure onset and offset patterns.

Our results demonstrated an involvement of the SN and SI dependent on the seizure onset and offset pattern. We found that seizures with both low amplitude fast activity (LAF) and high amplitude slow activity (HAS) onset patterns were associated with an increase in activity of the SN while the change in activity was limited to LAF seizures in the SI. However, the increase of HPC/SI coherence was similar for both type of onset, while the increase in HPC/SN coherence was specific to the farther-spreading LAF onset pattern. As for the role of the SN in seizure cessation, we observed that the coherence between the HPC/SN was reduced during burst suppression (BS) compared to other termination phases. Additionally, we found that this coherence returned to

normal levels after the seizure ended, with no significant difference in post-ictal periods among the three types of seizure offsets. This result suggests that the SN might be involved differently in the termination of the BS seizure pattern. This study constitutes the first demonstration of temporal lobe seizures entraining the SN in the primate brain. Moreover, these findings provide evidence that this entrainment is dependent on the seizure onset pattern and support the hypothesis that the SN might play a role in the maintenance and termination of some specific temporal lobe seizure.

1. Introduction

Epilepsy affects up 1% of the population with temporal lobe epilepsy (TLE) being the most common form of drug-resistant partial epilepsy [1]. For patients with drug resistant TLE, therapies include surgery to resect the epileptogenic tissue [2] or deep brain stimulation either at the focus (e.g., hippocampus) or within the same circuit (e.g., anterior nucleus of the thalamus [3-5]. While effective at reducing seizures, these therapies do not often result in complete seizure-freedom [6]. One way to improve treatments for TLE may be to account for the propagation of the seizure to other extralimbic structures. A major focus of human and animal studies on TLE network has been the limbic circuit and the structures composing the temporal lobe. However, there is also evidence suggesting an active role of the basal ganglia (BG) in the propagation and control of temporal lobe seizures. The BG network is a complex grouping of interconnected structures that receive diverse and topographically organized inputs from the cortex and thalamus [7,8] and is indirectly connected to the hippocampus (HPC), and amygdala [9-12]. Studies using intracranial recording have reported changes in oscillatory activity of BG structures including the putamen, pallidum, and caudate when temporal lobe seizures propagated beyond the temporal lobe [13,14] and in the putamen during temporal lobe seizures with ictal limb dystonia [15]. In addition, a PET study in patients with temporal and extratemporal epilepsy found a decreased uptake of [^{18}F] fluoro-L-dopa in the substantia nigra (SN), caudate, and putamen compared to healthy controls [16]. As one of the major outputs of the BG, the SN has been proposed to be a critical node responsible for the maintenance of temporal lobe seizures. In rodents, direct and indirect inhibition of the SN results in control of amygdala-kindled seizures [17-

[19]. Moreover, inhibition of the SN, particularly the anterior SN has been shown to be anti-ictogenic across a range of different models of focal and generalized seizures [20-26]. Similarly, low frequency stimulation of the SN has been found to suppress seizures in a cat penicillin (PCN) hippocampal seizure model [27]. Likewise, it has been shown that temporal lobe (TL) seizures can modulate activity in frontal cortical areas [28]. Studies have also consistently shown cognitive decline in patients with TLE [29]. Finally, TL seizures are associated with reduced connectivity between the temporal lobe and other cortical structures including the sensorimotor cortex (SI) [30]. Evidence also suggests that the network involved in temporal lobe seizure propagation may depend on the seizure dynamics. Most studies have focused their interest on seizure onset pattern [31-35] yet, studies on seizure termination may also provide valuable information to develop new personalized treatments to improve seizure outcome [36,37]. So far, studies on the relationship between extralimbic activity and the onset and offset dynamic of temporal lobe seizures have been limited[35]. Here, we characterize the involvement of the SN and SI during temporal lobe seizures induced in two nonhuman primates (NHP) and test the hypothesis that seizure differentially propagate through these neural circuits based on their onset and offset pattern.

2. Materials and Methods

2.1 Overview

We recorded local field potential (LFP) activity from the HPC and SN in two NHPs during temporal lobe seizures induced by local injection of penicillin in the HPC. Using these recordings, we characterized the changes in the oscillatory activity of the SN and

SI during the ictal period and how the coherence between the HPC and SN or SI changes depending on the seizure onset and offset pattern.

2.2 Animals, surgical procedures

Two rhesus macaques (macaca mulatta; 6-10 kg; one male, one female) were used for electrophysiological recording of the HPC and SN during temporal lobe seizures. The animals were pair-housed with other animals and had free access to food and water. All experiments were performed in accordance with the United States Public Health Service Policy on the humane care and use of laboratory animals, including the provisions of the "Guide for the Care and Use of Laboratory Animals" [38]. All studies were approved by the Institutional Biosafety and Animal Care and Use Committees of Emory University. The animals were first habituated to be handled by an experimenter and to sit in a primate chair. They then underwent aseptic surgery under isoflurane anesthesia (1-3%). Both animals had a recording chamber (Crist Instruments, Hagerstown, MD; inner chamber diameter 18 mm) implanted on their right side. The chamber was placed vertically in the coronal plane to permit simultaneous access to the HPC (for recording and injection) and the SN (for recording) (Figure 1B). NHP 2 had an additional electrode lead chronically implanted in the HPC (D08-15AM, 2 mm contact length, 1.5 mm between contacts, DIXI medical, France) and 2 ECoG electrodes located in the ipsilateral SI.

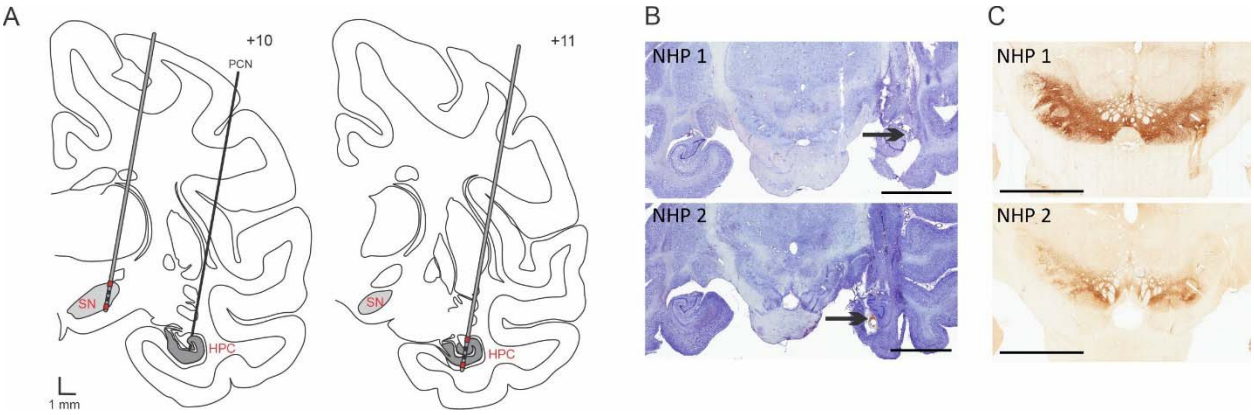

Figure 1: Electrode targeting. (A) Schematic representation of the electrode placement in the SN and PCN injection site in the HPC (left) as well as electrode placement in the HPC (right). The signal from the red contacts located in the ventral and dorsal part of the structure were subtracted from each other to obtain a bipolar recording signal in each structure. (B) Nissl stained sections showing the PCN injection site (black arrow) and electrode insertion tracts in the HPC for NHP 1 and 2. (C) TH staining showing the electrode tract in the SN for NHP 1 and 2. Abbreviations: Substantia nigra pars reticulata (SN), Hippocampus (HPC), Penicillin (PCN). Scale bars: B: 9 mm, C: 6 mm.

2.3 Seizure induction

Seizures were induced by an intrahippocampal injection of PCN diluted in sterile water (Penicillin G sodium salt (P3032), and sterile water for injection from Sigma-Aldrich, St. Louis, MI). Final concentration of PCN was 1,000 I.U./µl and for each session a dose of 6,000-10,000 I.U. of PCN was delivered at a rate of 1 µl/min using an injection system connected to a mechanical pump and microsyringe (CMA, Harvard Biosciences Inc, Krista, Sweden). At the end of the injection, the system was clamped to prevent any additional PCN leakage and carefully raised. Details of the model have been previously described [39]. Each PCN injection induced multiple spontaneous self-terminating seizures over a period of 4-6 hours and injections were separated by at least 2 weeks.

No spontaneous behavioral seizures were observed in between injections. The seizures induced were focal and not associated with obvious clinical motor symptoms. No oral automatisms were noted during ictal events.

2.4 Electrophysiological mapping and recording

Recordings were made while the animals were seated in a primate chair with their head fixed but body and limbs were free to move. Neural activity was recorded using a Cerebus data acquisition system (Blackrock Neurotech, Salt Lake City, UT). A post-surgery MRI was performed to orient the chamber and the locations of SN and HPC were confirmed by extracellular activity recorded with tungsten microelectrodes (FHC, Bowdoinham, ME; Z=0.5-1.0MΩ). The dura was pierced with a guide cannula and the electrode lowered into the brain with a microdrive (Nan instrument, Nof Hagalil, Israel). After delineating the SN and HPC borders, both structures were targeted for simultaneous LFP recordings with a 12-contact electrode consisting of 4 rings divided in 3 segments (outer diameter 600µm; inter-contact separation, 500µm; impedance, 25-35 kΩ; Heraeus Medical Components, St Paul, MN). On each recording day, one electrode was placed in the SN and the other in the HPC for simultaneous recordings from the two structures. The injection system was then lowered into the HPC, and seizures were induced. For NHP 2, ECoG from the SI was simultaneously recorded using a bipolar montage. LFP and ECoG signals were sampled at 2 kHz synchronized with the video of the animal.

2.5 Data processing and analysis

2.5.1 Pre-processing

Data were imported in Spike 2 interface (CED, Cambridge, UK) for offline annotation of ictal activity. Ictal activities were manually marked based on electrophysiological signal. We recorded 14 and 59 seizures respectively in NHP 1 and NHP 2. Subsequent analysis was performed using MATLAB (MATLAB R2021a, The Mathworks, Natick, MA, USA). The signal from each electrode contact was first normalized, then the 3 directional contacts positioned at the same level were averaged to mimic a configuration analogous to a clinical concentric 4x1 electrode. Finally, the signal from the contact located in the ventral part of the structure was subtracted from the signal in the dorsal part to obtain a bipolar recording signal in each structure (Figure 1A).

2.5.2 Seizure classification

The seizure onset and offset patterns were classified by a trained experimenter based on the three first and last seconds of the seizure.

Onset pattern: We identified 2 common seizure onset patterns. The low amplitude fast (LAF) activity onset pattern is characterized by low amplitude oscillations in the beta range that increases in amplitude as the seizure progresses. The high amplitude slow (HAS) activity onset pattern is characterized by high amplitude low frequency oscillations at seizure onset [32,40].

Offset pattern: We identified 3 characteristic seizure offset patterns. The arrhythmic offset pattern (ARR) is characterized by spike of irregular amplitudes, and mixed and oscillatory frequencies. The rhythmic offset pattern (RHY) is characterized by high amplitude spikes and consistent inter-spike intervals. The burst suppression offset

pattern (BS) is characterized by high amplitude, high frequency bursts interrupted by a period of suppressed activity [36,37,41].

The distribution of seizure onset and offset patterns was compared between animals using a Chi-square test.

2.5.3 Analysis

Simultaneous recordings from the HPC, SN, and SI were analyzed using the Chronux analysis software [42]. The individual power spectrogram and coherogram between signals was calculated using the multi-taper time-frequency method (moving window of 1 second and a window shift of 0.25 seconds). We extracted the power spectral density from the 3 seconds of signal preceding the seizure (pre-ictal), the 3 first seconds of the seizure onset and in the 3 last seconds of the seizure offset. The change in power and coherence were analyzed in 3 frequency bands: 1–7 Hz, 8–12 Hz and 13–25 Hz. These frequency bands were chosen based on the spectral activity of our PCN-induced seizure and previous clinical studies showing a cut off between LAF and HAS at 8 Hz [43].

All quantitative data were expressed as mean ± SEM. The statistical reliability of the differences between periods of interest (pre-ictal, onset, offset and post-ictal) was assessed either using a Friedman repeated measures test for paired quantitative data and Dunnett's test for post hoc analysis or a Wilcoxon Signed Rank test for paired quantitative data. Comparisons between seizure pattern were performed with a Mann-Whitney Rank Sum test. Statistical values were corrected for multiple comparisons using the Bonferroni method.

2.6 Histological verification of electrode placement

After completion of the experiment, the animals were euthanized with an overdose of pentobarbital sodium (100 mg/kg, i.v.) and transcardially perfused with cold oxygenated Ringer's solution, followed by a fixative containing 4% paraformaldehyde and 0.1% glutaraldehyde in a phosphate buffer (PB) solution. After perfusion, the brains were removed from the skull, cut coronally into 30 mm thick blocks, and post-fixed overnight in 4% paraformaldehyde. The blocks were then cryoprotected in ascending sucrose solution (10, 20 and 30% in PBS), cut into 50 µm-thick coronal sections using a freezing microtome and collected in series. Sections encompassing the SN from one series were immunostained using a tyrosine hydroxylase antibody, a marker of dopaminergic neurons to identify the position of the SN. Sections were rinsed in phosphate buffered saline (PBS; P3813, Sigma Aldrich, St. Louis, MO), permeabilized in PBS containing 0.3% hydrogen peroxide (H1009, Sigma Aldrich) and 0.1% of Triton-X (T8787, Sigma Aldrich) for 20 minutes with no shaking. Following several PBS rinses, sections were then incubated in 4% normal goat serum/PBS (NGS; 017-000121; Jackson Immunoresearch Laboratories) for 30 minutes at RT with shaking, rinsed in PBS, and incubated overnight in rabbit anti-TH antibodies (cat#P40101-150, Pel-Freez, Rogers, AR) at 4C with shaking. The next day, sections were rinsed and incubated in biotin SP conjugated donkey anti-rabbit IgG antibodies (cat#711-065-152, Jackson Immunoresearch Laboratories) in PBS containing 2% NGS at RT for 1hr with shaking, followed by additional rinses and an overnight incubation in avidin biotin complex (Vectastain Elite ABC kit HRP, standard, cat#PK-6100, Vector Laboratories). The next day sections were rinsed in PBS and incubated in a solution containing 3’3’-

diaminobezidine tetrahydrochloride hydrate (DAB; cat#D3737, Tokyo Chemical Industry) and hydrogen peroxide for 12 minutes at RT with shaking. Stained sections were mounted on gelatin coated glass slides, dried and coverslipped with Permount (SP15-100, Fischer Chemical). Sections through the SN from an adjacent series were mounted on glass slides and stained with cresyl violet to verify the electrode tract.

3. Results

3.1 Early involvement of the SN during TL seizure

We first analyzed all the seizures combined and found that for both animals, HPC activity was characterized by an increase in the 1–7 Hz, 8–12 Hz and 13–25 Hz frequency bands at seizure onset (Figure 2 and Supplementary Table 1). These oscillatory activities decreased at the end of the seizures but were still significantly higher in the 13–25 Hz range for both animals and in the 8–12 Hz for NHP 1 (Figure 2E). In contrast, while the power of the HPC in the low frequency band 1–7 Hz was increased at the beginning of the seizure, it returned to pre-ictal levels by the end of the seizure (Figure 2E). No change was observed in the low frequency activity of the SN but for both animals the power in the 8–12 Hz and 13–25 Hz frequency range was increased at the seizure onset (Figure 2E). These initial increases of oscillatory activity in the SN remained significantly higher during the rest of the seizure for NHP 2 but were no longer significant at the end of the seizure for NHP 1.

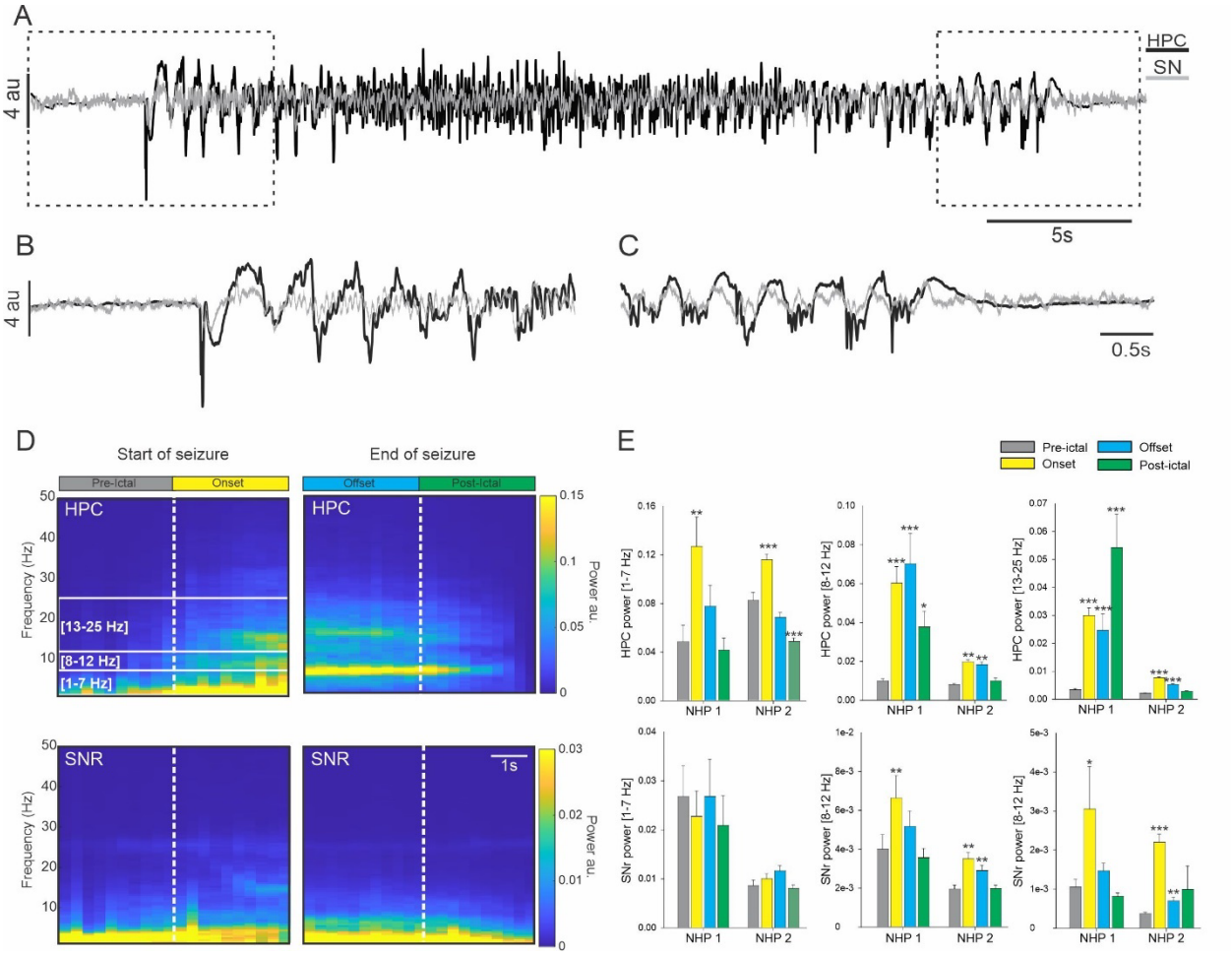

Figure 2: Power spectral density of the SN and HPC during seizures. (A) Example from NHP 1, of simultaneous recording obtained in the HPC and in the SN during a temporal lobe seizure with a focus on the start (B) and end (C) of the seizure. (D) Averaged spectral power obtained for NHP 1 in the HPC and SN at the start and end of the seizure. (E) Changes in the averaged power in the 1–7 Hz, 8–12 Hz and 13–25 Hz range in the HPC and SN for NHPs 1 and 2. Results are mean ± SEM. Statistical comparison performed with a Friedman repeated test and Tuckey for post hoc comparison with the pre-ictal values, *<0.05, **<0.01, ***<0.001.

3.2 Increase in coherence between the HPC and SN

For both animals and all seizures combined, the increase in coherence between the HPC and SN was limited to the 13–25 Hz frequency band at the seizure onset (Figure 3B). The coherence in the other frequency ranges examined was either decreased or unchanged (Supplementary Table 2).

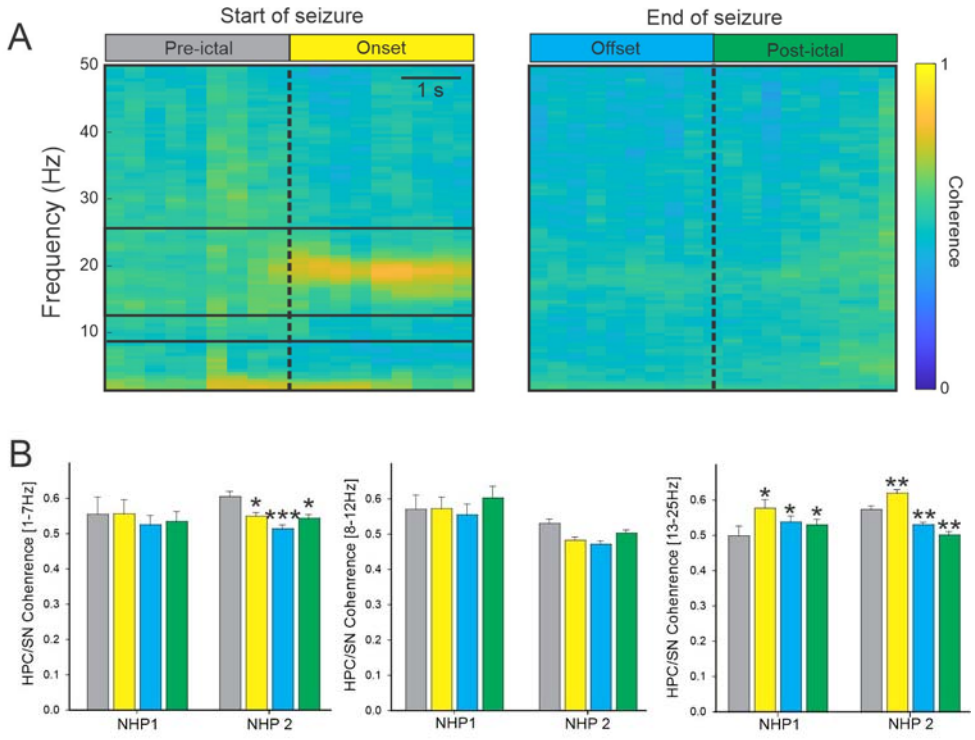

Figure 3: Coherence between HPC and SN during seizures. (A) Colormap representation of the averaged HPC/SN coherence obtained for NHP 2 at the start and end of the seizure. (B) The averaged HPC/SN coherence for NHP 1 and 2. Results are mean ± SEM. Statistical comparisons were performed with a Friedman repeated test and Tuckey for post hoc comparison with the values preceding the seizures, *<0.05, **<0.01, ***<0.001.

3.3 Change in HPC/SN activity depends on seizure onset pattern.

We identified a total of 18 seizures with an HAS onset pattern (22% and 25% of the seizures recorded in respectively NHP 1 and NHP 2) and 44 seizures with a LAF onset pattern (57% and 61% of the seizures recorded in NHP 1 and NHP 2). Eleven seizure onsets did not fall under either the HAS or LAS pattern and were therefore removed from subsequent analysis (21% and 14% respectively for NHP 1 and NHP 2). No difference was found in the proportion of seizure onset patterns between animals (Chi-square 0.22, Figure 4, A-C).

For both HAS and LAF onset seizures, the oscillatory power in the SN was increased in the 8–12 Hz and in the 13–25 Hz range (Figure 4D, Supplementary Table 3). The increase in HPC/SN coherence in the 13–25 Hz frequency range during the first 3 seconds of the seizure was specific to the LAF onset pattern (Figure 4E). No significant increase in HPC/SN coherence was found for the HAS onset pattern. However, the pre-ictal HPC/SN coherence was greater for the HAS seizures compared to the LAF seizures in the 1–7 Hz and 13–25 Hz range (Figure 4E, Supplementary Table 3) which might explained why we did not find an increase on the HAS seizure onset in the 13–25 Hz range.

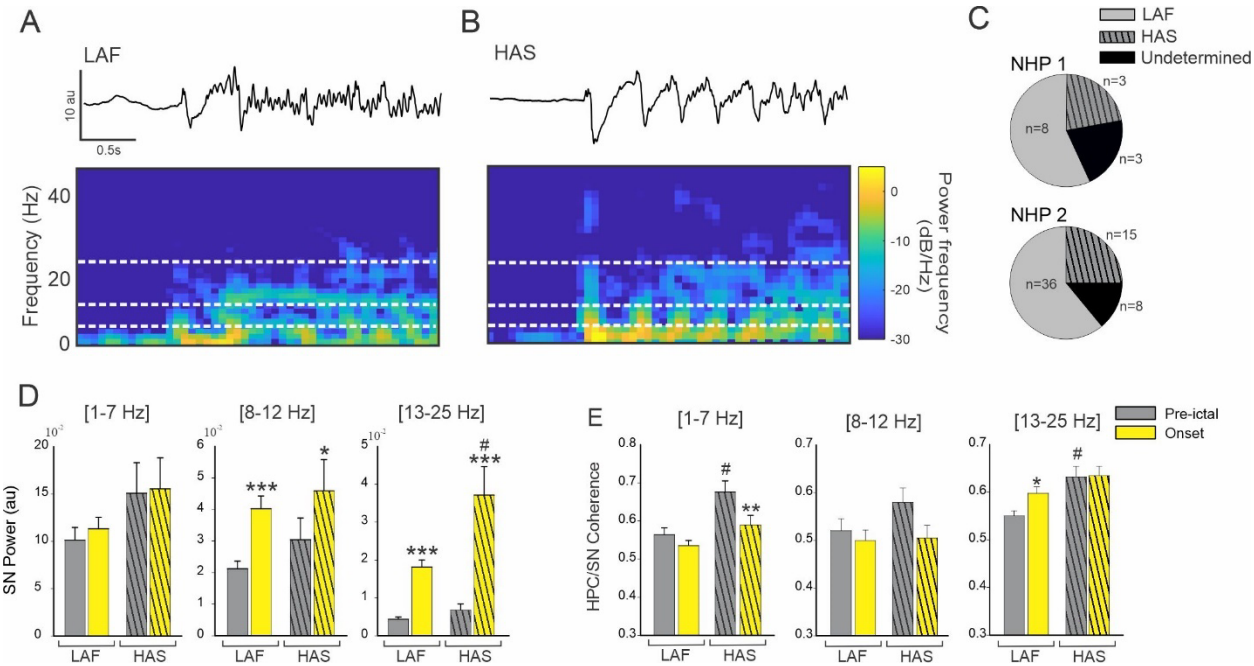

Figure 4: Effect of seizure onset pattern on HPC/SN activity. Example of typical LAF (A) and HAS (B) seizure showing HPC recording and corresponding spectral power. (C) Percentage of LAF, HAS, and undetermined seizures for NHP 1 and 2. (D) Changes in the averaged SN power and (E) HPC-SN coherence for LAF and HAS seizures. Results are mean ± SEM. Statistical testing for comparison of pre-ictal and onset periods was performed with a Wilcoxon signed rank test, *<0.05, **<0.01, ***<0.001. Comparisons between LAF and HAS seizures were performed with a Mann-Whitney Rank Sum test, # <0.05. Statistical values were corrected for multiple comparisons using the Bonferroni method.

3.4 Change in HPC/SN activity depends on seizure offset pattern.

We identified a total of 36 seizures with an ARR offset pattern, 21 with a RHY and 12 with a BS offset pattern. Four seizure offsets did not fall under either the ARR, RHY or BS pattern and were therefore removed from subsequent analysis (Figure 5, A-D). A

significant difference was found in the proportion of seizure offset patterns between animals (Figure 5D, Chi-square <0.001).

For all the offset patterns and all the frequency band analyzed, the oscillatory power in the SN was significantly decreased after the end of the seizure compared to the offset period (Figure 5E, Supplementary Table 4). For the ARR seizure offset pattern, we found an increase in HPC/SN coherence after the end of the seizure in the 8–12 Hz frequency range. We also found an increase of coherence after the end of the seizure for the BS offset in the 1-7 Hz and 13-25 Hz range, and interestingly during the offset periods the HPC/SN coherence in the BS seizure was lower compared to the ARR and RHY (Figure 5F and Supplementary Table 4). These results suggest that the SN might be involved in the ending of the BS seizures.

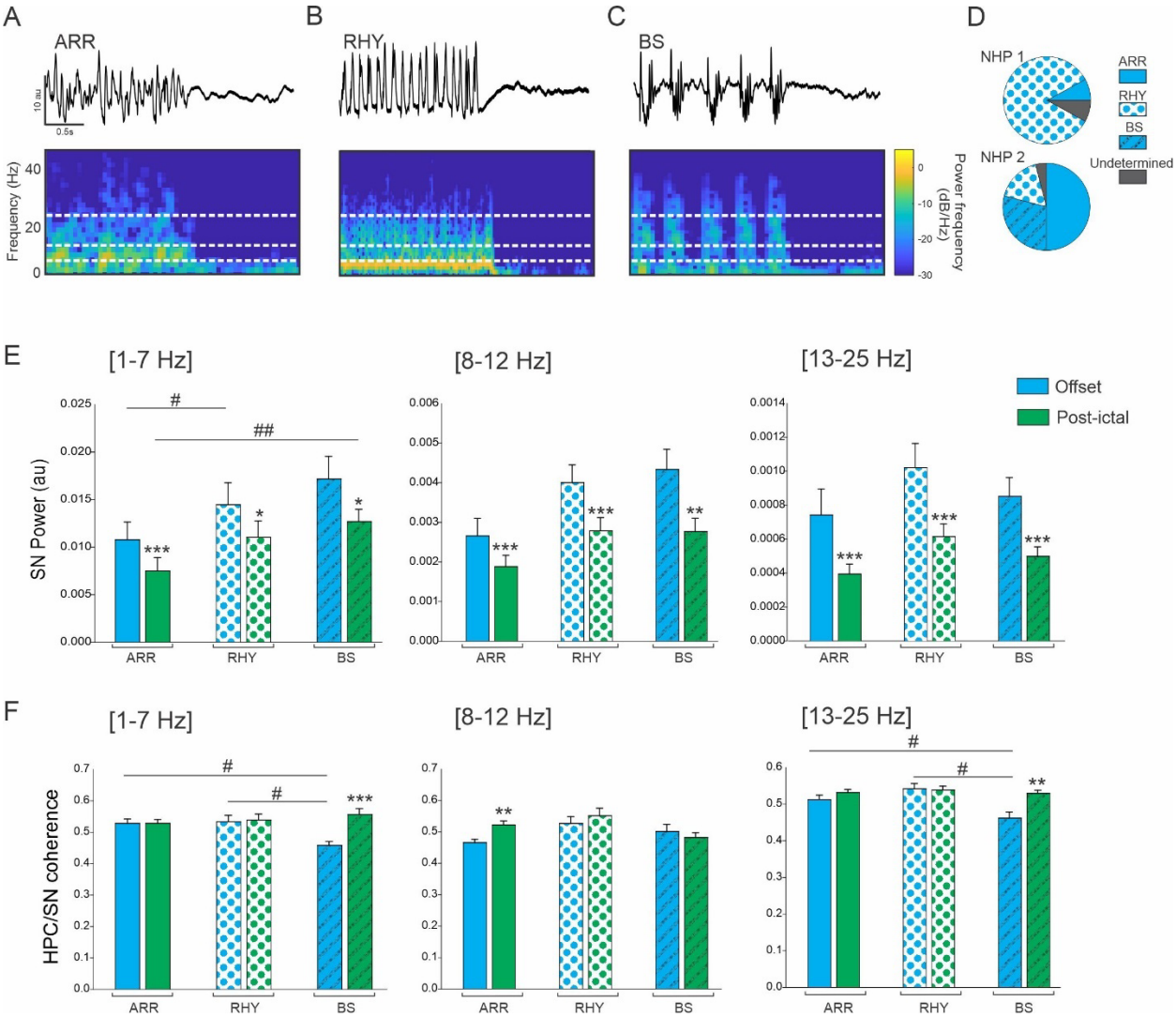

Figure 5: Effect of seizure offset pattern on HPC/SN activity. Example of typical ARR (A), RHY (B) and BS (C) seizure offset pattern. (D) Percentage of ARR, RHY, BS and undetermined seizures for NHP 1 and 2. (E) Changes in the averaged SN power and (F) HPC-SN coherence for LAF and HAS seizures. Results are mean ± SEM. Statistical comparison for comparison of offset and post-ictal period was performed with a Wilcoxon signed rank test, *<0.05, **<0.01, ***<0.001. Comparisons between ARR, RHY and BS seizures were performed with an ANOVA and Dunn's Post hoc test, # <0.05, ##<0.01. Statistical values were corrected for multiple comparison using the Bonferroni method.

3.5 Change in HPC/SI activity depends on seizure onset and offset pattern.

In NHP 2, we recorded the activity of the SI during 36 LAF and 15 HAS seizures (Figure 6A). We only found an increase of cortical oscillatory power at the beginning of the LAF seizures in the 1–7 Hz and 13–25 Hz ranges (Figure 6B-C Supplementary Table 5). Interestingly, we found that for all the frequency band analyzed, the cortical activity in the pre-ictal and onset period was significantly higher during LAF compared to HAS seizures which suggest that, on the contrary to the SN, the SI is more entrained by the LAF seizure type. The coherence between the HPC and SI was increased at the seizure onset in the 1-7 Hz range for both type of seizure and no difference in coherence was found between the LAF and HAS seizure onset. The coherence in the other frequency band were not significantly changed at the seizure onset (Supplementary Table 5).

We characterized the offset pattern of these seizures recorded in the SI and found 35 ARR, 9 RHY and 12 BS seizures offset pattern (Figure 6D-E). We found a decrease of cortical activity after the end of the seizure for the ARR and RHY pattern in the 8-12 and 13-25 Hz range (Figure 6D). In all the frequency range analyzed, cortical activity was lower during ARR seizure offset pattern compared to RHY and BS (in all the frequency range analyzed). The change in the coherence in the 1-7 Hz range at the end of ARR type and the HPC/SI coherence was overall higher during the RHY offset pattern. These results suggest that the SI might be more involved in the termination of ARR seizure than in the termination of RHY and BS seizure type.

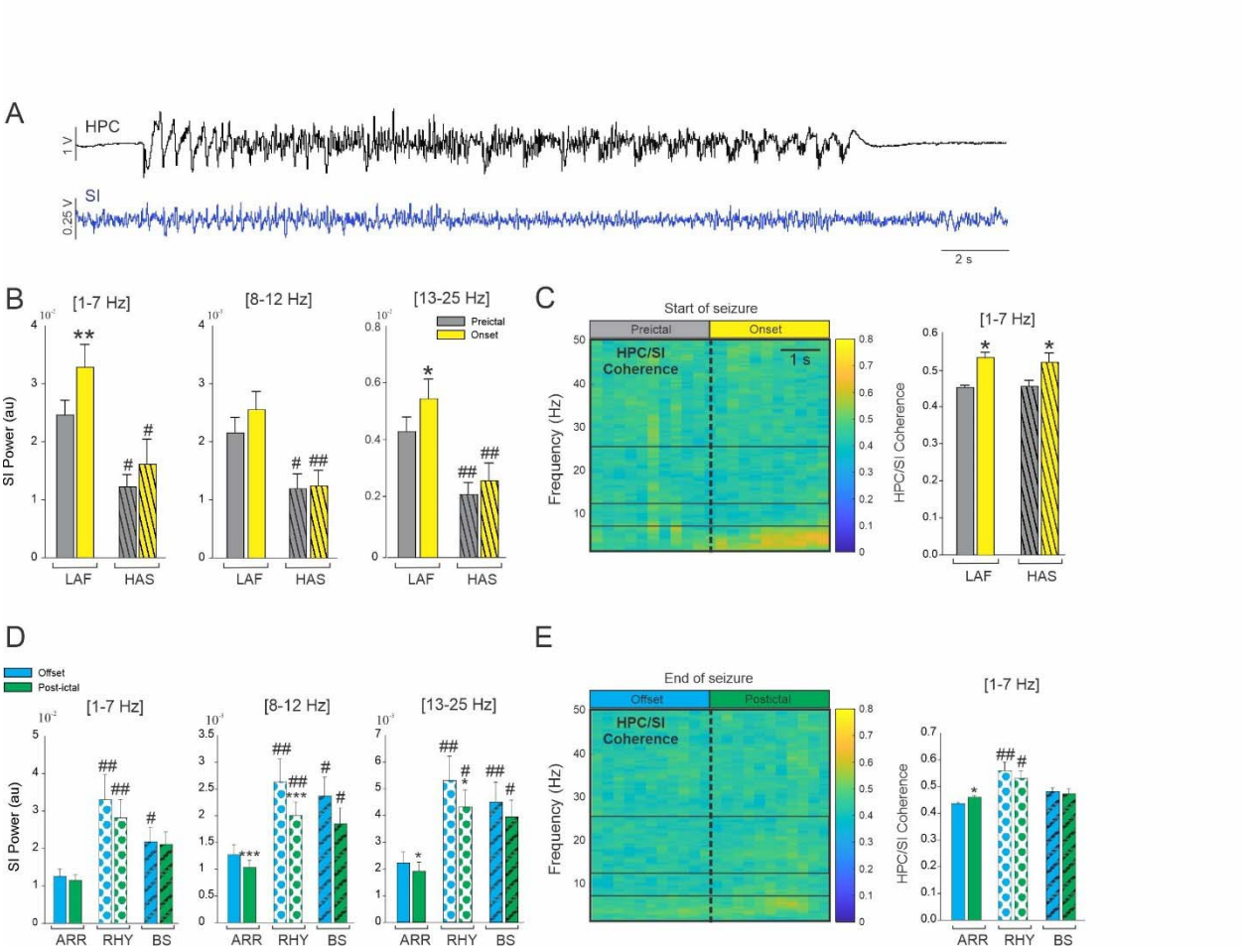

Figure 6: Influence of temporal lobe seizure onset and offset pattern on cortical activity. (A) Example of simultaneous recordings obtained from the HPC and the SI in NHP 2. (B) Changes in the averaged SI power for LAF and HAS seizures. (C) Colormap of the averaged HPC/SI coherence (LAF and HAS combined) and changes in the averaged HPC/SI coherence in the 1–7 Hz for LAF and HAS seizures. (D) Changes in the averaged SI power for ARR, RHY and BS seizures. (C) Colormap of the averaged HPC/SI coherence (LAF and HAS combined) and changes in the averaged HPC/SI coherence in the 1–7 Hz for LAF and HAS seizures. Results are mean ± SEM. Statistical comparisons between pre-ictal vs onset and offset vs postictal were performed with Wilcoxon signed rank test *<0.05, **<0.01 and ***<0.001. Comparisons between LAF and HAS seizures were performed with a Mann-Whitney Rank Sum test, and comparison between ARR, RHY and BS were performed with an ANOVA on rank

and Dunn's Post hoc test # <0.05, ##<0.01. Statistical values were corrected for multiple comparison using the Bonferroni method.

4. Discussion

In this study we recorded LFP activity in the HPC, SN, and SI during PCN-induced temporal lobe seizures. We found a global increase of activity in SN and HPC/SN coherence which confirm the involvement of the SN during temporal lobe seizures. Based on our results, it also seems the SN and SI involvement depend on the seizure onset and offset pattern. Seizures with both LAF and HAS onset patterns were associated with an increase of activity in the SN while the change in activity was limited to LAF seizures in the SI. However, the increase of HPC/SI coherence was similar for both type of onset, while the increase in HPC/SN coherence was specific to the farther-spreading LAF onset pattern. With regard to the involvement of the SN at the end of seizure, the coherence HPC/SN was lower during BS compared to other ending and this coherence was normalized at the end of this seizure with no difference in post-ictal phase between the 3 types of seizure offset. This result suggests that the SN might be involved in the termination of the BS seizure pattern. This study is the first demonstration of temporal lobe seizures entraining the SN in the primate brain. Moreover, these findings provide evidence that this entrainment is dependent on the seizure onset pattern and support the hypothesis that the SN might plays a role in the maintenance and termination of specific temporal lobe seizures.

4.1 The role of the SN in the control of seizures

As one of the major outputs of the BG, the SN has been proposed to be a critical node responsible for the maintenance of temporal lobe seizures. In rodents, direct and indirect inhibition of the SN results in control of amygdala-kindled seizures [17-19]. Likewise, inhibition of the SN, particularly the anterior SN has been shown to be anti-ictogenic across a range of different models of focal and generalized seizures [20-26]. Similarly, low frequency stimulation of the SN has been found to suppress seizures in a cat penicillin (PCN) hippocampal seizure model [27]. There is also a long history of clinical data implicating the BG in temporal and extratemporal seizures using electrophysiological recordings [13-15], measuring cerebral metabolism [44,45], and advanced fMRI analysis techniques [46]. To our knowledge, however, entrainment of the SN during a temporal lobe seizure has never been observed in the primate brain. Our finding that the coherence between the HPC and the SN is increased during the onset of temporal lobe seizures implicates the primate SN in TL seizures as in rodents and suggests that modulation of the non-human primate SN may have similar anti-seizure effects than in rodents.

4.2 Entrainment of the SN is dependent on seizure onset pattern.

Because of their importance in understanding ictogenesis and predicting treatment outcome, seizure onset patterns have recently drawn increasing attention [40,47,48]. The onset (1-5 seconds) of a seizure typically has a morphology consistent with one of several stereotyped onset patterns. Two of the most reported seizure onset patterns in patients with temporal lobe epilepsy are LAF and HAS onset patterns. The LAF seizure onset pattern is characterized by low amplitude oscillations in the beta to gamma range

that slowly increase as the seizure progresses, whereas the HAS onset pattern consists of high amplitude slow oscillations usually below the alpha range [32,33]. While both seizure onset patterns can arise from the same ictogenic circuit, seizures with the LAF onset pattern typically spread farther and have a larger seizure onset zone [31-34,49]. Similar to what has been described in clinical studies, our NHP model exhibited a prevalence of LAF onset pattern [32,48,50]. We found that both the LAF and HAS entrained the SI, but only LAF caused an increase in HPC/SN coherence. This finding corroborates clinical studies showing that LAF seizures are typically associated with a larger seizure onset zone and spread farther than HAS seizures in both temporal and extratemporal lobe seizures [31-34,49,51]. The finding that only the further-spreading LAF seizures influenced the SN would support the hypothesis that the SN plays a role in the propagation and generalization of seizures. However, we also found that the HPC/SN coherence during the pre-ictal period was higher for the HAS than for the LAF seizure type. This result is intriguing and should be investigated further as coherence between the HPC and other subcortical structure might convey information on seizure occurence.

4.3 Entrainment of the SN is dependent on seizure offset pattern.

Most studies on seizure dynamics have focused on onset pattern and propagation however, a better understanding of seizure termination may provide critical information regarding seizure mechanisms and open new approaches to treat status epilepticus [52]. Some papers have classified the seizure termination patterns in patients and the classification is very similar to the one we created for our NHP-PCN model [36,41,53,54]. As previously discussed, the role of SN in the termination of seizure has been investigated

in several rodent studies however no study has considered the implication of the SN in the context of different seizure termination patterns. Our results shows that the HPC/SN coherence was lower during BS compared to ARR and RHY seizures offset which might suggest that the SN might be involved differently in the termination of seizure depending on their pattern. Similarly, the thalamo-cortical synchronization has been found to vary depending on the offset pattern leading to the hypothesis that hypersynchronization might ultimately leads to the termination of a subtype of seizures [41].

4.4 Propagation network and cortical entrainment of temporal lobe seizures

Multiple studies have shown the propagation of temporal lobe seizures to the SN although the pathway, mechanism, and role of the BG therein remains unclear. It has been suggested that BG activity is modulated by seizures via cortical areas [13,55], and that the HPC-cortico-striatal connection is the entrance pathway leading to the entrainment of the BG. In support of this theory, studies have shown a preventative effect of GABA antagonist and dopamine agonist injections in the striatum [56-58]. Our results also agree with this hypothesis of cortical recruitment, as the LAF seizure that were associated with an increase in HPC/SN coherence were also associated with an increase in HPC/SI coherence. However, while we did not find a difference in HPC/SI coherence for both type of seizure onset, the SI power during HAS seizure was significantly lower than during LAF seizure at seizure onset but also in the pre-ictal state. It is possible that while both type of seizure might propagated similarly to the SI,

the indirect and direct BG pathway might be engaged differently based on the SI oscillatory activity [59].

4.4 Limitations.

Although these results demonstrate the implication of the BG in temporal lobe epilepsy and the relevance of the seizure patterns when studying pathways and mechanisms, as is often the case in NHP studies the relatively small number of animals is a limitation. Additionally, in our study, the recordings were obtained from the posterior part of the SN on both animals. Although it is well known that the topographical segregation of efferent and afferent connections in the SN is even more pronounced in the NHP than in the rodent [60], we were unable to characterize any regional variability in SN seizure activity because - to limit neural tissue damage caused by acutely targeting deep structures - we only obtained recordings from one SN location. Future studies can address this by recording and modulating different parts of the SN to evaluate the potential topography of seizure regulation in the NHP. Along this line, we acknowledge that without comprehensive EEG recordings, we cannot conclude that the entrainment of the SN was mediated through cortical recruitment and it is possible that the entrainment of the SN could also be due to seizure propagation via another pathway [61].

Finally, our seizure onset and offset classification was only based on the recording done at the seizure focus and the activity in other location were not taken into account. Thus, for the offset pattern we did not evaluate if the seizure was ending synchronously or asynchronously across the brain [31]. A more detailed distinction of the

seizure patterns could be made in the future but would require additional seizures and recordings site [36,37].

5. Conclusion

This work demonstrates the implication of the SN in temporal lobe seizures in NHP. In addition, we showed that the SN and cortex entrainment were dependent on the seizure onset and offset pattern. These results confirm the idea that seizures arising from the same focus might involve different pathways depending on their pattern of progression and termination. Finally, this study re-opens new lines of research into the control of temporal lobe seizures outside of the limbic network.

References:

1. Semah F, Picot MC, Adam C, et al. Is the underlying cause of epilepsy a major prognostic factor for recurrence? *Neurology*. 1998;51(5):1256. doi:10.1212/WNL.51.5.1256

2. Wiebe S, Blume WT, Girvin JP, Eliasziw M. A Randomized, Controlled Trial of Surgery for Temporal-Lobe Epilepsy. *New England Journal of Medicine*. 2001;345(5):311-318. doi:10.1056/nejm200108023450501

3. Salanova V, Sperling MR, Gross RE, et al. The SANTE study at 10 years of follow-up: Effectiveness, safety, and sudden unexpected death in epilepsy. *Epilepsia*. Jun 2021;62(6):1306-1317. doi:10.1111/epi.16895

4. Cukiert A, Cukiert CM, Burattini JA, Mariani PP, Bezerra DF. Seizure outcome after hippocampal deep brain stimulation in patients with refractory temporal lobe epilepsy: A prospective, controlled, randomized, double-blind study. *Epilepsia*. Oct 2017;58(10):1728-1733. doi:10.1111/epi.13860

5. Nair DR, Laxer KD, Weber PB, et al. Nine-year prospective efficacy and safety of brain-responsive neurostimulation for focal epilepsy. *Neurology*. Sep 1 2020;95(9):e1244-e1256. doi:10.1212/WNL.0000000000010154

6. Spencer S, Huh L. Outcomes of epilepsy surgery in adults and children. *The Lancet Neurology*. 2008;7(6):525-537. doi:10.1016/s1474-4422(08)70109-1

7. Wichmann T, Delong MR. Anatomy and physiology of the basal ganglia: relevance to Parkinson's disease and related disorders. *Handb Clin Neurol*. 2007;83:1-18. doi:10.1016/S0072-9752(07)83001-6

8. Lanciego JL, Luquin N, Obeso JA. Functional neuroanatomy of the basal ganglia. *Cold Spring Harb Perspect Med*. Dec 1 2012;2(12):a009621. doi:10.1101/cshperspect.a009621

9. Haber SN, Lynd E, Klein C, Groenewegen HJ. Topographic organization of the ventral striatal efferent projections in the rhesus monkey: an anterograde tracing study. *J Comp Neurol*. Mar 08 1990;293(2):282-98.

10. Jones DL, Mogenson GJ. Nucleus accumbens to globus pallidus GABA projection: electrophysiological and iontophoretic investigations. *Brain Res*. Apr 21 1980;188(1):93-105.

11. Yang CR, Mogenson GJ. Electrophysiological responses of neurones in the nucleus accumbens to hippocampal stimulation and the attenuation of the excitatory responses by the mesolimbic dopaminergic system. *Brain Res*. Dec 17 1984;324(1):69-84.

12. Kahn I, Shohamy D. Intrinsic connectivity between the hippocampus, nucleus accumbens, and ventral tegmental area in humans. *Hippocampus*. Mar 2013;23(3):187-92. doi:10.1002/hipo.22077

13. Rektor I, Kuba R, Brazdil M. Interictal and ictal EEG activity in the basal ganglia: an SEEG study in patients with temporal lobe epilepsy. *Epilepsia*. Mar 2002;43(3):253-62. doi:10.1046/j.1528-1157.2002.28001.x

14. Rektor I, Kuba R, Brazdil M, Halamek J, Jurak P. Ictal and peri-ictal oscillations in the human basal ganglia in temporal lobe epilepsy. *Epilepsy Behav*. Mar 2011;20(3):512-7. doi:10.1016/j.yebeh.2011.01.003

15. Kuba R, Rektor I, Brazdil M. Ictal limb dystonia in temporal lobe epilepsy. an invasive video-EEG finding. *Eur J Neurol*. Nov 2003;10(6):641-9. doi:10.1046/j.1468-1331.2003.00684.x

16. Bouilleret V, Semah F, Chassoux F, et al. Basal ganglia involvement in temporal lobe epilepsy: a functional and morphologic study. *Neurology*. Jan 15 2008;70(3):177-84. doi:10.1212/01.wnl.0000297514.47695.48

17. Deransart C, Le BT, Marescaux C, Depaulis A. Role of the subthalamo-nigral input in the control of amygdala-kindled seizures in the rat. *Brain Res*. Oct 5 1998;807(1-2):78-83. doi:10.1016/s0006-8993(98)00745-8

18. McNamara JO, Galloway MT, Rigsbee LC, Shin C. Evidence implicating substantia nigra in regulation of kindled seizure threshold. *J Neurosci*. Sep 1984;4(9):2410-7.

19. Shin C, Silver JM, Bonhaus DW, McNamara JO. The role of substantia nigra in the development of kindling: pharmacologic and lesion studies. *Brain Research*. 1987/06/02/ 1987;412(2):311-317. doi:https://doi.org/10.1016/0006-8993(87)91138-3

20. Garant DS, Gale K. Substantia nigra-mediated anticonvulsant actions: role of nigral output pathways. *Exp Neurol*. Jul 1987;97(1):143-59. doi:10.1016/0014-4886(87)90289-5

21. Moshe SL, Garant DS, Sperber EF, Veliskova J, Kubova H, Brown LL. Ontogeny and topography of seizure regulation by the substantia nigra. *Brain Dev*. 1995;17 Suppl:61-72. doi:10.1016/0387-7604(95)90074-8

22. Xu SG, Garant DS, Sperber EF, Moshe SL. Effects of substantia nigra gamma-vinyl-GABA infusions on flurothyl seizures in adult rats. *Brain Res*. Dec 6 1991;566(1-2):108-14. doi:10.1016/0006-8993(91)91687-v

23. Wicker E, Beck VC, Kulick-Soper C, et al. Descending projections from the substantia nigra pars reticulata differentially control seizures. *Proc Natl Acad Sci U S A*. Dec 26 2019;116(52):27084-27094. doi:10.1073/pnas.1908176117

24. Paz JT, Chavez M, Saillet S, Deniau JM, Charpier S. Activity of ventral medial thalamic neurons during absence seizures and modulation of cortical paroxysms by the nigrothalamic pathway. *J Neurosci*. Jan 24 2007;27(4):929-41. doi:10.1523/JNEUROSCI.4677-06.2007

25. Depaulis A, Snead OC, 3rd, Marescaux C, Vergnes M. Suppressive effects of intranigral injection of muscimol in three models of generalized non-convulsive epilepsy induced by chemical agents. *Brain Res*. Sep 25 1989;498(1):64-72. doi:10.1016/0006-8993(89)90399-5

26. Depaulis A, Vergnes M, Marescaux C, Lannes B, Warter JM. Evidence that activation of GABA receptors in the substantia nigra suppresses spontaneous spike-and-wave discharges in the rat. *Brain Res*. May 10 1988;448(1):20-9. doi:10.1016/0006-8993(88)91097-9

27. Sabatino M, Gravante G, Ferraro G, Vella N, La Grutta G, La Grutta V. Striatonigral suppression of focal hippocampal epilepsy. *Neurosci Lett*. Apr 10 1989;98(3):285-90. doi:10.1016/0304-3940(89)90415-1

28. Englot DJ, Yang L, Hamid H, et al. Impaired consciousness in temporal lobe seizures: role of cortical slow activity. *Brain*. Dec 2010;133(Pt 12):3764-77. doi:10.1093/brain/awq316

29. Stretton J, Thompson PJ. Frontal lobe function in temporal lobe epilepsy. *Epilepsy Res*. Jan 2012;98(1):1-13. doi:10.1016/j.eplepsyres.2011.10.009

30. Haneef Z, Lenartowicz A, Yeh HJ, Levin HS, Engel Jr J, Stern JM. Functional connectivity of hippocampal networks in temporal lobe epilepsy. *Epilepsia*. 2014;55(1):137-145. doi:https://doi.org/10.1111/epi.12476

31. Perucca P, Dubeau F, Gotman J. Intracranial electroencephalographic seizure-onset patterns: effect of underlying pathology. *Brain*. Jan 2014;137(Pt 1):183-96. doi:10.1093/brain/awt299

32. Velasco AL, Wilson CL, Babb TL, Engel J, Jr. Functional and anatomic correlates of two frequently observed temporal lobe seizure-onset patterns. *Neural Plast*. 2000;7(1-2):49-63. doi:10.1155/NP.2000.49

33. Alarcon G, Binnie CD, Elwes RD, Polkey CE. Power spectrum and intracranial EEG patterns at seizure onset in partial epilepsy. *Electroencephalogr Clin Neurophysiol*. May 1995;94(5):326-37. doi:10.1016/0013-4694(94)00286-t

34. Wetjen NM, Marsh WR, Meyer FB, et al. Intracranial electroencephalography seizure onset patterns and surgical outcomes in nonlesional extratemporal epilepsy. *J Neurosurg*. Jun 2009;110(6):1147-52. doi:10.3171/2008.8.JNS17643

35. Ilyas A, Toth E, Chaitanya G, Riley K, Pati S. Ictal high-frequency activity in limbic thalamic nuclei varies with electrographic seizure-onset patterns in temporal lobe epilepsy. *Clin Neurophysiol*. May 2022;137:183-192. doi:10.1016/j.clinph.2022.01.134

36. Shokooh LA, Toffa DH, Pouliot P, Lesage F, Nguyen DK. Intracranial EEG seizure onset and termination patterns and their association. *Epilepsy Res*. Oct 2021;176:106739. doi:10.1016/j.eplepsyres.2021.106739

37. Salami P, Borzello M, Kramer MA, Westover MB, Cash SS. Quantifying seizure termination patterns reveals limited pathways to seizure end. *Neurobiol Dis*. Apr 2022;165:105645. doi:10.1016/j.nbd.2022.105645

38. Garber J, Barbee R, Bielitzki J, et al. Guide for the Care and Use of Laboratory Animals (8th ed.). *Washington (DC): National Academies Press (US); 2011* 2011;doi:NBK54050 [bookaccession]

39. Sherdil A, Chabardes S, Guillemain I, et al. An on demand macaque model of mesial temporal lobe seizures induced by unilateral intra hippocampal injection of penicillin. *Epilepsy Res*. May 2018;142:20-28. doi:10.1016/j.eplepsyres.2018.03.008

40. Wang Y, Trevelyan AJ, Valentin A, Alarcon G, Taylor PN, Kaiser M. Mechanisms underlying different onset patterns of focal seizures. *PLoS Comput Biol*. May 2017;13(5):e1005475. doi:10.1371/journal.pcbi.1005475

41. Evangelista E, Benar C, Bonini F, et al. Does the Thalamo-Cortical Synchrony Play a Role in Seizure Termination? *Front Neurol*. 2015;6:192. doi:10.3389/fneur.2015.00192

42. Mitra P, Bokil H. *Observed Brain Dynamics*. Oxford University Press; 2008.

43. Dolezalova I, Brazdil M, Hermanova M, Horakova I, Rektor I, Kuba R. Intracranial EEG seizure onset patterns in unilateral temporal lobe epilepsy and their relationship to other variables. *Clin Neurophysiol*. Jun 2013;124(6):1079-88. doi:10.1016/j.clinph.2012.12.046

44. Bertti P, Dal-Col ML, Wichert-Ana L, et al. The neurobiological substrates of behavioral manifestations during temporal lobe seizures: a neuroethological and ictal SPECT correlation study. *Epilepsy Behav*. Mar 2010;17(3):344-53. doi:10.1016/j.yebeh.2009.12.030

45. Sperling MR, Gur RC, Alavi A, et al. Subcortical metabolic alterations in partial epilepsy. *Epilepsia*. Mar-Apr 1990;31(2):145-55. doi:10.1111/j.1528-1167.1990.tb06299.x

46. Rektor I, Tomcik J, Mikl M, Marecek R, Brazdil M, Rektorova I. Association between the basal ganglia and large-scale brain networks in epilepsy. *Brain Topogr*. Apr 2013;26(2):355-62. doi:10.1007/s10548-012-0272-8

47. Lagarde S, Buzori S, Trebuchon A, et al. The repertoire of seizure onset patterns in human focal epilepsies: Determinants and prognostic values. *Epilepsia*. Jan 2019;60(1):85-95. doi:10.1111/epi.14604

48. Jimenez-Jimenez D, Nekkare R, Flores L, et al. Prognostic value of intracranial seizure onset patterns for surgical outcome of the treatment of epilepsy. *Clin Neurophysiol*. Feb 2015;126(2):257-67. doi:10.1016/j.clinph.2014.06.005

49. Park SA, Lim SR, Kim GS, et al. Ictal electrocorticographic findings related with surgical outcomes in nonlesional neocortical epilepsy. *Epilepsy Research*. 2002/02/01/ 2002;48(3):199-206. doi:https://doi.org/10.1016/S0920-1211(02)00006-2

50. Ogren JA, Bragin A, Wilson CL, et al. Three-dimensional hippocampal atrophy maps distinguish two common temporal lobe seizure-onset patterns. *Epilepsia*. Jun 2009;50(6):1361-70. doi:10.1111/j.1528-1167.2008.01881.x

51. Boido D, Jesuthasan N, de Curtis M, Uva L. Network dynamics during the progression of seizure-like events in the hippocampal-parahippocampal regions. *Cereb Cortex*. Jan 2014;24(1):163-73. doi:10.1093/cercor/bhs298

52. Zubler F, Steimer A, Gast H, Schindler KA. Seizure termination. *Int Rev Neurobiol*. 2014;114:187-207. doi:10.1016/B978-0-12-418693-4.00008-X

53. Bauer PR, Thijs RD, Lamberts RJ, et al. Dynamics of convulsive seizure termination and postictal generalized EEG suppression. *Brain*. Mar 1 2017;140(3):655-668. doi:10.1093/brain/aww322

54. Amzica F. Basic physiology of burst-suppression. *Epilepsia*. Dec 2009;50 Suppl 12:38-9. doi:10.1111/j.1528-1167.2009.02345.x

55. Haut SR, Albin RL. Dopamine and epilepsy: hints of complex subcortical roles. *Neurology*. Sep 9 2008;71(11):784-5. doi:10.1212/01.wnl.0000325637.38931.27

56. Turski L, Cavalheiro EA, Bortolotto ZA, Ikonomidou-Turski C, Kleinrok Z, Turski WA. Dopamine-sensitive anticonvulsant site in the rat striatum. *J Neurosci*. Nov 1988;8(11):4027-37.

57. Turski L, Diedrichs S, Klockgether T, et al. Paradoxical anticonvulsant activity of the gamma-aminobutyrate antagonist bicuculline methiodide in the rat striatum. *Synapse*. Jan 1991;7(1):14-20. doi:10.1002/syn.890070103

58. Cavalheiro EA, Bortolotto ZA, Turski L. Microinjections of the gamma-aminobutyrate antagonist, bicuculline methiodide, into the caudate-putamen prevent amygdala-kindled seizures in rats. *Brain Res*. May 19 1987;411(2):370-2.

59. Vuong J, Devergnas A. The role of the basal ganglia in the control of seizure. *J Neural Transm (Vienna)*. Mar 2018;125(3):531-545. doi:10.1007/s00702-017-1768-x

60. Parent A, Mackey A, Smith Y, Boucher R. The output organization of the substantia nigra in primate as revealed by a retrograde double labeling method. *Brain Res Bull*. Apr 1983;10(4):529-37. doi:10.1016/0361-9230(83)90151-x

61. Spencer SS. Neural networks in human epilepsy: evidence of and implications for treatment. *Epilepsia*. Mar 2002;43(3):219-27.

Supplement

Supplementary Table 1: Mean ± SEM values obtained in the pre-ictal, onset, offset and post-ictal periods in the HPC and SN for NHP1 and NHP 2. Statistical comparison performed with a Friedman repeated test and Dunnett's for post hoc comparison with the values preceding the seizures, *<0.05, **<0.01, ***<0.001. Numbers in bold represent results consistent for both animals.

		NHP 1				**NHP 2**			
		Pre-ictal	Onset	Offset	Post-ictal	Pre-ictal	Onset	Offset	Post-ictal
HPC	[1–7Hz]	0.049±0.014	**0.127±0.024****	0.078±0.017	0.042±0.010	0.082±0.006	**0.116±0.005*****	0.069±0.004	**0.049±0.002*****
	[8–12Hz]	0.010±0.001	**0.060±0.008*****	**0.070±0.015*****	**0.038±0.008***	0.008±0.001	**0.020±0.001*****	**0.018±0.001*****	0.010±0.001
	[13–25Hz]	0.003±0.001	**0.030±0.003*****	**0.025±0.006****	**0.054±0.012*****	0.002±0.001	**0.008±0.001*****	**0.005±0.001*****	0.028±0.001
SN	[1–7Hz]	0.027±0.006	0.023±0.005	0.027±0.007	0.021±0.006	0.009±0.001	0.010±0.001	0.012±0.001	0.008±0.001
	[8–12Hz]	0.004±0.001	**0.006±0.001***	0.005±0.001	0.004±0.001	0.002±0.001	**0.004±0.001*****	0.003±0.001**	0.002±0.001
	[13–25Hz]	0.001±0.001	**0.003±0.001***	0.001±0.001	0.001±0.001	0.001±0.001	**0.002±0.001*****	0.001±0.001**	0.001±0.001

Supplementary Table 2: Mean ± SEM values of the HPC/SN coherence obtained before, at the beginning and the end of the seizure for NHP1 and NHP 2. Statistical comparison performed with a Friedman repeated test and Dunnett's for post hoc comparison with the pre-ictal values, *<0.05, **<0.01, ***<0.001. Numbers in bold represent results consistent for both animals.

		NHP 1				NHP 2			
		Pre-ictal	Onset	Offset	Post-ictal	Pre-ictal	Onset	Offset	Post-ictal
HPC-SN	[1–7Hz]	0.55±0.05	0.56±0.04	0.52±0.03	0.53±0.03	0.60±0.01	0.55±0.01*	0.51±0.01***	0.53±0.01*
	[8–12Hz]	0.57±0.04	0.57±0.03	0.55±0.03	0.60±0.03	0.53±0.01	0.48±0.01	0.47±0.01	0.50±0.01
	[13–25Hz]	0.50±0.03	**0.55±0.02***	0.54±0.01*	0.60±0.03*	0.53±0.01	**0.62±0.01*****	0.53±0.01**	0.50±0.01**

Supplementary Table 3: Mean ± SEM spectra values and coherence obtained in the pre-ictal and onset periods in the HPC and SN for LAF and HAS onset patterns. Statistical comparison performed with a Wilcoxon Signed Rank test for paired quantitative data, *<0.05, **<0.01, ***<0.001. Comparisons between LAF and HAS seizures were performed with a Mann-Whitney Rank Sum test (# <0.05). Statistical values were corrected for multiple comparison using Bonferroni correction.

		LAF (n=44)		HAS (n=18)	
		Pre-ictal	Onset	Pre-ictal	Onset
HPC	[1–7Hz]	0.063±0.006	0.107±0.006 ***	0.104±0.014#	0.137±0.009**#
	[8–12Hz]	0.007±0.001	0.029±0.004***	0.010±0.001	0.023±0.002***
	[13–25]	0.002±0.001	0.013±0.002***	0.003±0.001	0.009±0.001***
SN	[1–7Hz]	0.010±0.001	0.011±0.001	0.015±0.003	0.016±0.003
	[8–12Hz]	0.002±0.001	0.004±0.001***	0.003±0.001	0.005±0.001*
	[13–25Hz]	0.001±0.001	0.002±0.001***	0.001±0.001	0.004±0.001***#
HPC/SN	[1–7Hz]	0.56±0.02	0.54±0.01	0.68±0.03#	0.59±0.02**
	[8–12Hz]	0.52±0.01	0.50±0.01	0.58±0.03	0.50±0.03
	[13–25Hz]	0.55±0.01	0.59±0.01*	0.63±0.02#	0.63±0.02

Supplementary Table 4: Mean ± SEM spectra values and coherence obtained in the offset and post-ictal periods in the HPC and SN for ARR, RHY and BS offset patterns. Statistical comparison performed with a Wilcoxon Signed Rank test for paired quantitative data, *<0.05, **<0.01, ***<0.001.

		ARR (n=36)		RHY (n=44)		BS (n=12)	
		Offset	Post-ictal	Offset	Post-ictal	Offset	Post-ictal
HPC	[1–7Hz]	0.067±0.004	0.047±0.003***	0.079±0.011	0.047±0.006***	0.056±0.006	0.047±0.007
	[8–12Hz]	0.021±0.002	0.011±0.002***	0.046±0.011	0.025±0.006***	0.015±0.001	0.009±0.002***
	[13–25]	0.006±0.002	0.003±0.001***	0.017±0.004	0.034±0.009**	0.005±0.001	0.002±0.001***
SN	[1–7Hz]	0.011±0.002	0.007±0.001***	0.014±0.002	0.011±0.002*	0.017±0.002	0.013±0.001*
	[8–12Hz]	0.003±0.001	0.002±0.001***	0.004±0.001	0.003±0.001***	0.004±0.001	0.003±0.001***
	[13–25]	0.0006±0.002	0.0003±0.001***	0.001±0.001	0.0006±0.001***	0.0008±0.001	0.0005±0.003***
HPC/SN	[1–7Hz]	0.53±0.014	0.53±0.012	0.53±0.020	0.55±0.019	0.46±0.011	0.56±0.019***
	[8–12Hz]	0.47±0.011	0.52±0.013**	0.53±0.021	0.55±0.024	0.050±0.02	0.048±0.015
	[13–25]	0.51±0.012	0.53±0.008	0.54±0.014	0.54±0.011	0.46±0.016	0.53±0.008***

Supplementary Table 5: Mean ± SEM values obtained before, at the beginning and the end of the seizures in the SI for LAF and HAS onset patterns. Statistical comparison performed with a Friedman repeated test and Dunnett's for post hoc comparison with the values preceding the seizures, *<0.05, **<0.01, ***<0.001. Comparisons between LAF and HAS seizures were performed with a Mann-Whitney Rank Sum test (# <0.05). Statistical values were corrected for multiple comparison using Bonferroni correction.

		LAF (n=36)		HAS (n=15)	
		Pre-ictal	Onset	Pre-ictal	Onset
SI	[1–7Hz]	0.024±0.002	0.033±0.004 **	0.012±0.002###	0.016±0.004##
	[8–12Hz]	0.021±0.003	0.026±0.003	0.012±0.002#	0.012±0.003##
	[13–25]	0.004±0.001	0.005±0.001*	0.002±0.001##	0.003±0.001##
HPC/SI	[1–7Hz]	0.46±0.01	0.53±0.01***	0.46±0.02	0.52±0.02*
	[8–12Hz]	0.44±0.01	0.43±0.01	0.43±0.02	0.41±0.01
	[13–25Hz]	0.44±0.01	0.43±0.01	0.43±0.02	0.42±0.01

Supplementary Table 6: Mean ± SEM values obtained before, at the beginning and the end of the seizures in the SI for LAF and HAS onset patterns. Statistical comparison performed with a Friedman repeated test and Dunnett's for post hoc comparison with the values preceding the seizures, *<0.05, **<0.01, ***<0.001. Comparisons between LAF and HAS seizures were performed with a Mann-Whitney Rank Sum test (# <0.05). Statistical values were corrected for multiple comparison using Bonferroni correction.

		ARR (n=35)		RHY (n=9)		BS (n=12)	
		Offset	Post-ictal	Offset	Post-ictal	Offset	Post-ictal
SI	[1–7Hz]	0.012±0.002	0.011±0.002	0.033±0.007	0.028±0.005	0.022±0.004	0.021±0.003
	[8–12Hz]	0.013±0.002	0.010±0.001	0.026±0.004	0.020±0.002	0.024±0.003	0.018±0.003
	[13–25]	0.002±0.001	0.002±0.001	0.005±0.001	0.004±0.001	0.004±0.001	0.004±0.001
HPC/SI	[1–7Hz]	0.44±0.01	0.46±0.01	0.56±0.03	0.53±0.03	0.48±0.02	0.47±0.02
	[8–12Hz]	0.41±0.01	0.43±0.01	0.44±0.01	0.47±0.01	0.43±0.01	0.45±0.01
	[13–25Hz]	0.42±0.01	0.43±0.01	0.44±0.01	0.47±0.01	0.42±0.01	0.44±0.01